

# Crystallization characteristics of nitrogen-doped $\text{Sb}_2\text{Te}_3$ films for PRAM application

Myoung Sub Kim<sup>a</sup>, Sung Hyuk Cho<sup>a</sup>, Suk Kyoung Hong<sup>b</sup>,  
Jae Sung Roh<sup>b</sup>, Doo Jin Choi<sup>a,\*</sup>

<sup>a</sup>Department of Ceramic Engineering, Yonsei University, 134 Shinchon-dong, Sudaemun-ku, Seoul 120-749, Republic of Korea

<sup>b</sup>Memory R&D Division, Hynix Semiconductor Inc., San 136-1, Amiri, Bubal-eup, Ichon-si, Kyoungki-do 467-701, Republic of Korea

Available online 2 October 2007

## Abstract

The  $\text{Sb}_2\text{Te}_3$  film is an attractive candidate for phase change random access memory (PRAM) due to its rapid crystallization speed. However, the  $\text{Sb}_2\text{Te}_3$  film has unstable amorphous phase. In order to improve the phase stability and easy reamorphization, the nitrogen-doped  $\text{Sb}_2\text{Te}_3$  films were proposed. The characteristics of nitrogen-doped  $\text{Sb}_2\text{Te}_3$  films were investigated using the secondary ion mass spectroscopy (SIMS), 4-point probe technique, X-ray diffraction and static test. The nitrogen doping caused the increase of crystallization temperature and sheet resistance of the  $\text{Sb}_2\text{Te}_3$  films. Furthermore, the crystallization speed of nitrogen-doped  $\text{Sb}_2\text{Te}_3$  film was superior to the  $\text{Ge}_2\text{Sb}_2\text{Te}_5$  film.

© 2007 Elsevier Ltd and Techna Group S.r.l. All rights reserved.

**Keywords:** A. Films; C. Electrical properties;  $\text{Sb}_2\text{Te}_3$ ; PRAM; Sputter

## 1. Introduction

The PRAM technology [1] stores information using rapid and reversible phase transition of chalcogenide material between a crystalline phase, which has low resistance and high reflectivity, and an amorphous phase, which is highly resistive and lowly reflective. Among the chalcogenide materials, the  $\text{GeTe-Sb}_2\text{Te}_3$  pseudobinary films, such as the  $\text{Ge}_2\text{Sb}_2\text{Te}_5$  (GST), have been widely researched as a candidate for a rewritable optical disk and PRAM application [2]. Many research groups have focused on the easy reamorphization that is obtained by controlling the electrical resistance and melting temperature of chalcogenide material [3], or making novel cell structure [4], rapid crystallization and enhanced phase stability for PRAM application. In the previous report, the crystallization time of alloys on the pseudobinary line reduces as GeTe content decrease [5]. Thus, the  $\text{Sb}_2\text{Te}_3$  has the advantage of rapid crystallization speed. However, the  $\text{Sb}_2\text{Te}_3$  has the unstable amorphous phase due to its low crystallization temperature and the data retention is not guaranteed for PRAM

application. In this paper, the nitrogen doping effect in the  $\text{Sb}_2\text{Te}_3$  films was investigated since the nitrogen doping method increases the crystallization temperature and electrical resistance in crystalline phase [6]. It is expected that the nitrogen-doped  $\text{Sb}_2\text{Te}_3$  films improve the stability of amorphous phase and property of reamorphization without loss of the crystallization speed.

## 2. Experimental procedure

The films were deposited on three different substrates, Si for SIMS analysis,  $\text{SiO}_2/\text{Si}$  for XRD analysis and glass for 4-point probe and Static test by DC magnetron sputtering system using  $\text{Sb}_2\text{Te}_3$  (99.99%) or  $\text{Ge}_2\text{Sb}_2\text{Te}_5$  (99.99%) composite target at room temperature. The plasma power and working pressure were maintained at 12 W and  $9.0 \times 10^{-3}$  torr, respectively. The nitrogen-doped  $\text{Sb}_2\text{Te}_3$  films were obtained by changing the ratio of nitrogen gas (99.9999%) to argon (99.999%) gas flow. The nitrogen gas flow changed from 0 sccm to 6 sccm since nitrogen doping of 6 sccm is thought as optimum condition for PRAM application. Total gas flow was fixed at 40 sccm to maintain process vacuum at  $9.0 \times 10^{-3}$  torr which is most stable condition of plasma state and deposition. The as-deposited films were annealed at the various temperatures

\* Corresponding author.

E-mail address: [drchoidj@yonsei.ac.kr](mailto:drchoidj@yonsei.ac.kr) (D.J. Choi).

for 20 min under vacuum condition (below  $3.0 \times 10^{-6}$  torr) with heating rate of  $10^\circ\text{C}/\text{min}$ .

The compositions of un-doped  $\text{Sb}_2\text{Te}_3$  and  $\text{Ge}_2\text{Sb}_2\text{Te}_5$  films were confirmed by X-ray photoelectron spectroscopy at 2B1 beam line in Pohang Accelerator Laboratory (PLS). The relative contents of nitrogen were analyzed by secondary ion mass spectroscopy (SIMS, CAMECA IMS-6F). The SIMS analysis was performed with a  $\text{Cs}^+$  primary ion source of 10 keV accelerating voltage. The electrical property changes caused by nitrogen doping effects were observed by measuring the sheet resistance by the 4-point probe (CMT-SR2000N). The crystal structures of films were also investigated by X-ray diffraction (XRD, DMAX-III A, Rigaku, Japan) analysis using  $\text{Cu K}\alpha$  ( $\lambda = 0.15405$  nm), and the crystallization speed was observed by laser irradiation using static tester (Nanostorage Co. Ltd., Korea).

### 3. Results and discussion

Fig. 1 shows the relative secondary ion intensities of  $^{14}\text{N}$  at the different nitrogen gas flow rate, in the range of sputtering time from 10 s to 100 s. The profiles of  $^{14}\text{N}$  in ST(2), ST(4) and ST(6) films, which were deposited at the nitrogen gas flow rates of 2 sccm, 4 sccm and 6 sccm, respectively, show uniform slope in comparison with ST(0) film which was deposited without nitrogen gas flow and the relative nitrogen contents increased as nitrogen gas flow rate increased.

The sheet resistance changes of  $\text{Sb}_2\text{Te}_3$  films annealed at the various temperatures for 20 min are shown in Fig. 2. The sheet resistance of as-deposited ST(0) film was about  $7.0 \times 10^5 \Omega_{\text{sq}}$  and abruptly decreased above the annealing temperature of  $100^\circ\text{C}$ . However, the sheet resistances of ST(2), ST(4), and ST(6) films were more than  $10^7 \Omega_{\text{sq}}$  in the low annealing temperature range ( $\sim 100^\circ\text{C}$ ) and began to decrease sharply above  $120^\circ\text{C}$ ,  $140^\circ\text{C}$ , and  $180^\circ\text{C}$ , respectively. Furthermore, the ST(4) and ST(6) films showed higher sheet resistance than the ST(0) film at all annealing temperature. It is thought that these results were related to the crystallization phenomena of

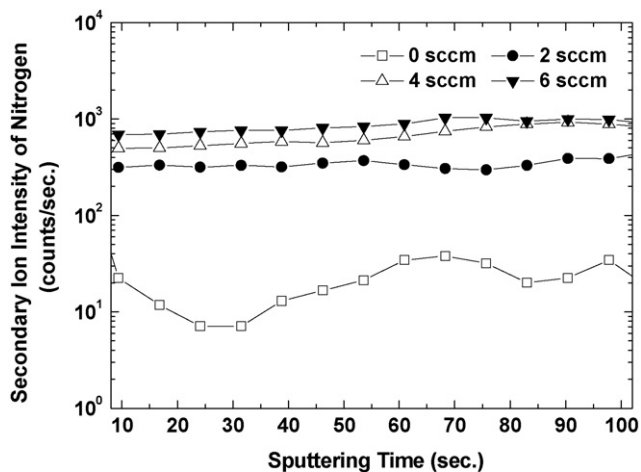


Fig. 1. The relative secondary ion intensities of  $^{14}\text{N}$  at the different nitrogen gas flow rate, in range of the sputtering time from 10 s to 100 s measured by SIMS depth profiles.

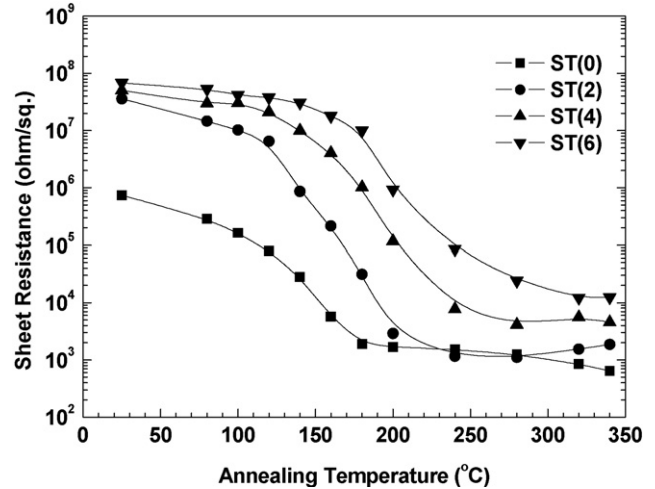


Fig. 2. Sheet resistance changes of ST(0), ST(2), ST(4) and ST(6) films annealed at the various temperatures for 20 min.

nitrogen-doped  $\text{Sb}_2\text{Te}_3$  films. Accordingly, these films were investigated by the XRD analysis.

XRD analysis showed that the as-deposited ST(0) film was a crystalline phase due to the near metallic nature of  $\text{Sb}_2\text{Te}_3$  previously reported [7]. However, it showed that those as-deposited ST(2), ST(4) and ST(6) films were amorphous phases [8]. The higher sheet resistances of nitrogen-doped  $\text{Sb}_2\text{Te}_3$  films in as-deposited state (see Fig. 2) are caused by these amorphous phase.

The XRD patterns of ST(0), ST(2), ST(4) and ST(6) films annealed at  $180^\circ\text{C}$  are shown in Fig. 3. The ST(0) film clearly maintained a crystalline phase, and ST(2) and ST(4) films were a mixture of amorphous phase and a crystalline phase. This means that ST(2) and ST(4) films started phase transition from amorphous phase to crystalline phase at this annealing temperature. On the other hand, the ST(6) film still remained as an amorphous phase despite annealing at  $180^\circ\text{C}$ . The reason is probably that nitrogen atoms in  $\text{Sb}_2\text{Te}_3$  film remain as nitrides like the Sb-N and Te-N [9]. It is known that the nitrides inhibit

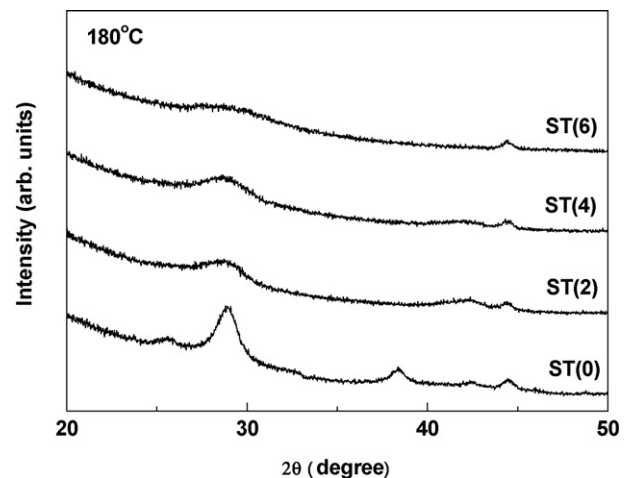


Fig. 3. XRD patterns of ST(0), ST(2), ST(4) and ST(6) films annealed at  $180^\circ\text{C}$  for 20 min.

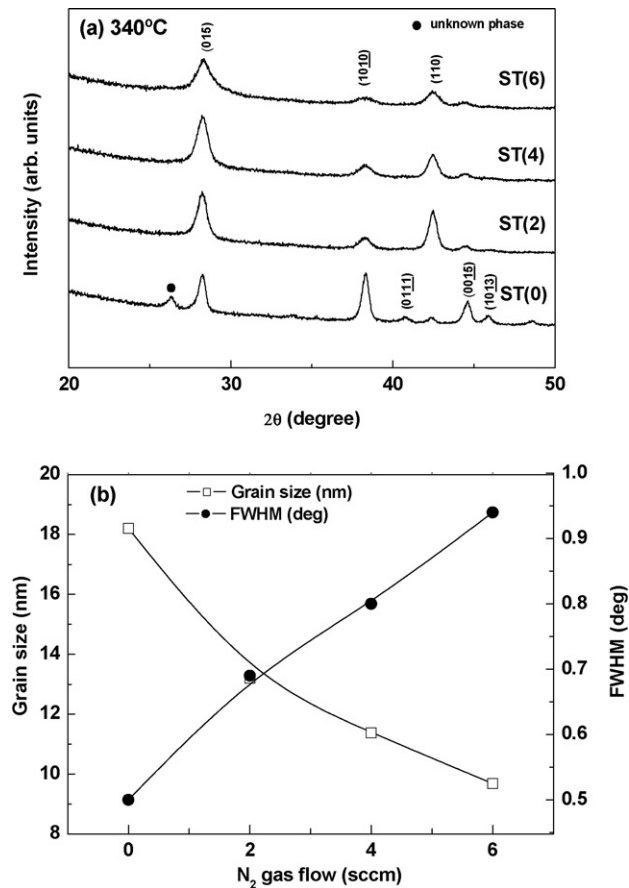


Fig. 4. XRD patterns of (a) ST(0), ST(2), ST(4) and ST(6) films annealed at 340 °C. (b) Shows changes of grain size and FWHM as a function of nitrogen gas flow rate.

grain growth during the crystallization of  $\text{Sb}_2\text{Te}_3$  films [10]. According to these results, the nitrogen doping into the  $\text{Sb}_2\text{Te}_3$  film has an advantage of stable operation for PRAM device since it inhibits the easy and fast crystallization of  $\text{Sb}_2\text{Te}_3$  film [11]. This can be a solution that complements the demerit of  $\text{Sb}_2\text{Te}_3$  film which has the poor stability of amorphous phase due to low crystallization temperature. The phase stability of nitrogen-doped  $\text{Sb}_2\text{Te}_3$  films is as good as the  $\text{Ge}_2\text{Sb}_2\text{Te}_5$  films [6].

Fig. 4(a) shows the XRD patterns of ST(0), ST(2), ST(4) and ST(6) films annealed at 340 °C. They showed the crystalline phase which has a rhombohedral crystal structure assigned by JCPDS data (15-0874). The relative intensities of nitrogen-doped  $\text{Sb}_2\text{Te}_3$  films were similar to each other, while the (1 0 10) peak was the most intense in case of the ST(0) film. The change of preferred orientation in the ST(0) film through annealing process is in good agreement with the previous report [12]. The grain size of  $\text{Sb}_2\text{Te}_3$  films was calculated based on the full-width at half maximum (FWHM) of (0 1 5) preferred orientation using the Scherrer equation. Fig. 4(b) shows the changes of grain size as a function of nitrogen gas flow rate. The grain size of  $\text{Sb}_2\text{Te}_3$  films decreased with increasing nitrogen gas flow rate. The decrease of grain size causes the increase of grain boundaries and the disturbance of electron movement [13]. This is the reason why the sheet resistances of crystallized ST(4) and ST(6) films is higher than

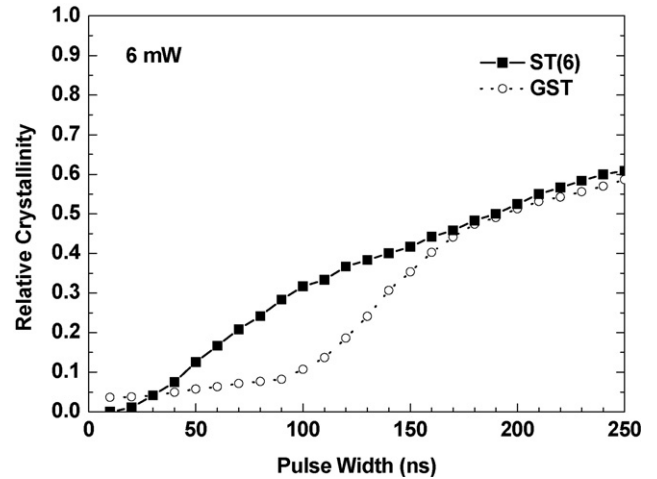


Fig. 5. Pulse width dependence on the relative crystallinity of ST(6) and GST films with 6 mW laser power.

the ST(0) film (see Fig. 2). The higher sheet resistance in crystalline phase enhances the joule heating for the phase transition. Thus, this result shows that the nitrogen doping into the  $\text{Sb}_2\text{Te}_3$  film can accomplish the reset current reduction for the PRAM operation [3].

The optical reflectivity changes of ST(6) and  $\text{Ge}_2\text{Sb}_2\text{Te}_5$  (GST) films were investigated for the comparison of crystallization speed using the static tester with the laser power from 1 mW to 20 mW and pulse width from 10 ns to 250 ns. The optical reflectivity of ST(0) film was not mentioned since the as-deposited ST(0) film was the crystalline phase. As previously reported, the optical reflectivity ( $R$ ) is a perfect linear dependence on the crystallinity ( $f$ ) [14]. Therefore, the relative crystallinity was discussed by the following expression:

$$f_{\text{relative}} = \left( \frac{R_{f,x} - R_{i,\text{aver.}}}{R_{f,\text{max}} - R_{i,\text{aver.}}} \right) \quad (1)$$

where  $R_{f,x}$  is the final reflectivity at the specific pulse width, and  $R_{f,\text{max}}$  and  $R_{i,\text{aver.}}$  are the final maximum reflectivity and initial average reflectivity, respectively. Fig. 5 shows the pulse width dependence on the relative crystallinity of ST(6) and GST films at the laser power of 6 mW. In Fig. 5, the threshold time which is required time for starting the crystallization of as-deposited amorphous film was about 20 ns in the ST(6) film, while the GST film showed the threshold time of about 90 ns. Also, it is confirmed that at the higher laser power (12 mW), the ST(6) film showed the shorter threshold time (10 ns) than the GST film (40 ns). It shows that the ST(6) film has faster crystallization process than the GST film regardless of the laser power, and the threshold time decreases with increasing laser power. This means that the ST(6) film is superior to the GST film for the fast set operation of PRAM device.

#### 4. Conclusions

Effects of the nitrogen doping on the crystallization characteristics of the  $\text{Sb}_2\text{Te}_3$  films were investigated. The

nitrogen-doped  $\text{Sb}_2\text{Te}_3$  films were deposited at various nitrogen gas flow rates using DC magnetron sputtering system. The relative contents of nitrogen were confirmed by SIMS analysis. The nitrogen doping increased the crystallization temperature and sheet resistance. These results indicate that the nitrogen doping into  $\text{Sb}_2\text{Te}_3$  films improved phase stability and easy reamorphization. The ST(6) which is considered as the most suitable nitrogen content in this paper, showed the shorter crystallization threshold time than the GST film. This means that the nitrogen-doped  $\text{Sb}_2\text{Te}_3$  films have advantages of the high speed and low power consumption for PRAM application.

### Acknowledgements

This work was supported by the second stage of Brain Korea 21 project in 2006. This work was supported by Hynix Semiconductor Inc. of Korea. The experiments at the PLS were supported in part by the MOST and the POSTECH.

### References

- [1] A.L. Lacaita, Phase change memories: State-of-the-art, challenges and perspectives, *Solid-State Electron.* 50 (2006) 24–31.
- [2] A.V. Kolobov, P. Fons, A.I. Frenkel, A.L. Ankudinov, J. Tominaga, T. Uruga, Understanding the phase-change mechanism of rewritable optical media, *Nat. Mater.* 3 (2004) 703–708.
- [3] H. Horii, J.H. Yi, J.H. Park, Y.H. Ha, I.G. Baek, S.O. Park, Y.N. Hwang, S.H. Lee, Y.T. Kim, K.H. Lee, U-In Chug, J.T. Moon, A novel cell technology using N-doped  $\text{GeSbTe}$  films for phase change RAM, in: Symposium on VLSI Technology Digest of. Technical Papers, 2003.
- [4] M.H.R. Lankhorst, B.W.S.M.M. Ketelaars, R.A.M. Wolters, Low-cost and nanoscale non-volatile memory concept for future silicon chips, *Nat. Mater.* 4 (2005) 347–352.
- [5] N. Yamada, E. Ohno, K. Nishiuchi, N. Akahira, M. Takao, Rapid-phase transitions of  $\text{GeTe-Sb}_2\text{Te}_3$  pseudobinary amorphous thin films for an optical disk memory, *J. Appl. Phys.* 69 (5) (1991) 2849–2856.
- [6] S.M. Kim, J.H. Jun, D.J. Choi, S.K. Hong, Y.J. Park, A study on the crystallization behavior of nitrogen doped  $\text{Ge}_2\text{Sb}_2\text{Te}_5$  thin film, *Jpn. J. Appl. Phys.* 44 (2005) L208–L210.
- [7] R.S. Rawat, P. Arun, A.G. Vedeshwar, Y.L. Lam, M.H. Liu, P. Lee, S. Lee, A.C.H. Huan, Effect of argon ion irradiation on  $\text{Sb}_2\text{Te}_3$  films in a dense plasma focus device, *Mat. Res. Bull.* 35 (2000) 477–486.
- [8] S. Fujimori, S. Yagi, H. Yamazaki, N. Funakoshi, Crystallization process of  $\text{Sb-Te}$  alloy films for optical storage, *J. Appl. Phys.* 64 (3) (1988) 1000–1004.
- [9] R. Kojima, S. Okabayashi, T. Kashihara, K. Horai, T. Matsunaga, E. Ohno, N. Yamada, T. Ohta, Nitrogen doping effect on phase change optical disks, *Jpn. J. Appl. Phys.* 37 (1998) 2098–2103.
- [10] T.H. Jeong, M.R. Kim, H. Seo, J.W. Park, C. Yeon, Crystal structure and microstructure of nitrogen-doped  $\text{Ge}_2\text{Sb}_2\text{Te}_5$  thin film, *Jpn. J. Appl. Phys.* 39 (2000) 2775–2779.
- [11] S.W. Ryu, J.H. Oh, B.J. Choi, S.-Y. Hwang, S.K. Hong, C.S. Hwang, H.J. Kim,  $\text{SiO}_2$  incorporation effects in  $\text{Ge}_2\text{Sb}_2\text{Te}_5$  films prepared by magnetron sputtering for phase change random access memory devices, *Electrochem. Solid-State Lett.* 9 (8) (2006) G259–G261.
- [12] A.E. Abkena, O.J. Barteltb, Sputtered  $\text{Mo/Sb}_2\text{Te}_3$  and  $\text{Ni/Sb}_2\text{Te}_3$  layers as back contacts for  $\text{CdTe/CdS}$  solar cells, *Thin Solid Films* 403–404 (2002) 216–222.
- [13] S.M. Kim, M.J. Shin, D.J. Choi, K.N. Lee, S.K. Hong, Y.J. Park, Electrical properties and crystal structures of nitrogen-doped  $\text{Ge}_2\text{Sb}_2\text{Te}_5$  thin film for phase change memory, *Thin Solid Films* 469–470 (2004) 322–326.
- [14] D.-H. Kim, F. Merget, M. Laurenzis, P.H. Bolivar, H. Kurz, Electrical percolation characteristics of  $\text{Ge}_2\text{Sb}_2\text{Te}_5$  and Sn doped  $\text{Ge}_2\text{Sb}_2\text{Te}_5$  thin films during the amorphous to crystalline phase transition, *J. Appl. Phys.* 97 (2005), 083538–083538-5.